J Incl Phenom Macrocycl Chem (2007) 57:511–517
DOI 10.1007/s10847-006-9242-7

ORIGINAL ARTICLE

Cisapride/β-cyclodextrin complexation: stability constants, thermodynamics, and guest–host interactions probed by ^{1}H-NMR and molecular modeling studies

M. M. Al Omari · M. B. Zughul · J. Eric D. Davies · A. A. Badwan

Received: 15 May 2006 / Accepted: 20 October 2006 / Published online: 10 January 2007

Abstract Phase solubility techniques were used to obtain the complexation parameters of cisapride (**Cisp**) with β-cyclodextrin (β-CD) in aqueous 0.05 M citrate buffer solutions. From the UV absorption spectra and the pH solubility profile, two basic pK_as were estimated: p$K_{a(1+)}$ = 8.7 and p$K_{a(2+)}$ < 2. The inherent solubility (S_o) of **Cisp** was found to increase as pH decreases, but is limited by the solubility product of **the** **Cisp**H$^+$·citrate^{1-} salt at low pH (pK_{sp} = 3.0). Cisp forms soluble 1:1 and 1:2 **Cisp**/β-CD complexes. A quantitative measure of the hydrophobic effect (desolvation) contribution to 1:1 complex formation was obtained from the linear variation of free energy of 1:1 **Cisp**/β-CD complex formation ($\Delta G_{11} = -RT \ln K_{11} < 0$) with that of the inherent solubility of **Cisp** ($\Delta G_{S_o} = -RT \ln S_o > 0$). The results show that the hydrophobic character of **Cisp** contributes about 35% of the total driving force to 1:1 complex formation (slope = –0.35), while other factors, including specific interactions, contribute –10.6 kJ/mol (intercept). Protonated 1:1 **Cisp**/β-CD complex formation at pH 6.0 is driven by favorable enthalpy ($\Delta H°$ = –9 kJ/mol) and entropy ($\Delta S°$ = 51 J/mol K) changes. In contrast, inherent **Cisp** solubility is impeded by unfavorable enthalpy ($\Delta H°$ = 12 kJ/mol) and entropy ($\Delta S°$ = 90 J/mol K) changes. ^{1}H-NMR spectra in D_2O and molecular mechanical studies indicate the formation of inclusion complexes. The dominant driving force for neutral **Cisp**/β-CD complexation in vacuo was predominantly van der Waals with very little electrostatic contribution.

Keywords Cisapride · Cyclodextrin · Hydrophobic effect · Thermodynamics · ^{1}H-NMR · Molecular mechanical modeling

M. M. Al Omari · A. A. Badwan
The Jordanian Pharmaceutical Manufacturing Company, Naor, Jordan

M. B. Zughul (✉)
Department of Chemistry, University of Jordan, Amman, Jordan
e-mail: mbzughul@ju.edu.jo

J. E. D. Davies
Deparment of Environmental Science, Lancaster University, Lancaster, England

Introduction

Cyclodextrins have been used to enhance the solubility of water-insoluble drugs through the formation of more soluble inclusion complexes in aqueous solutions [1, 2].

The effect of various factors such as pH, buffer composition, and addition of different ionic strength adjusters on inclusion complex formation have been reported [3–6]. For example, protonated basic drugs were found to have a lower complexation tendency than the neutral species [3, 4]. The anionic species of acidic celecoxib has lower complex formation constant than the neutral species [5]. Also protonated and anionic species of amphoteric sildenafil have a lower tendency to complex than neutral sildenafil [6]. Organic buffers were reported to interact more with cyclodextrins than inorganic buffers [5, 7]. The solubility of some dihydropyridine derivatives in aqueous 2-hydroxypropyl-β-cyclodextrin (HP-β-CD) was found to be lower in citrate than phosphate buffers, an effect related to a lower solubility product of the citrate salt

[8]. Ternary complexes of ketoconazole/acid/β-CD including citric and hydrochloric acid showed some pH dependence of their dissolution profiles [9].

This work reports the results of an investigation of the effect of pH and temperature on the inclusion complexation of **Cisp** with β-CD. UV Absorption spectroscopy and phase solubility techniques were used to obtain estimates of pK_as and complex formation constants. A quantitative evaluation of the contributions of hydrophobic effects, specific interactions, entropy and enthalpy to complex stability is also presented. ^{1}H-NMR spectral studies and molecular modeling of guest–host interactions were carried out to explore inclusion complex formation and possible sites of guest–host interactions (Scheme 1).

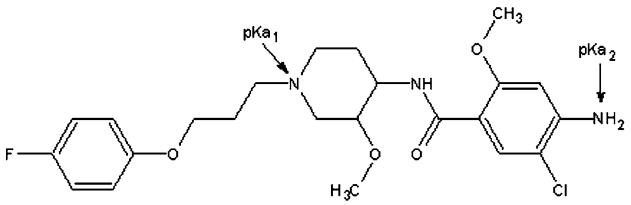

Scheme 1 Chemical structure of cisapride (**Cisp**)

Materials and methods

Materials

Cisp and β-CD were obtained from The Jordanian Pharmaceutical Manufacturing Company (JPM). All other chemicals were of analytical or HPLC grades obtained from Merck/Germany and Surechem/England. The hydrochloride salt of **Cisp** and its β-CD complex were prepared by dissolving **Cisp** (3 mmol) in sufficient amounts of water containing amount of HCl (3 mmol) and β-CD (6 mmol). The samples were freeze-dried and the solids were collected. Doubly distilled deionised water was used throughout.

Methods

Instrumentation

The instruments used were UV/Visible spectrophotometer (Du-650i, Beckman, USA), Thermostatic shaker (1086, GFL, Germany), pH-meter (3030, Jenway, England), Freeze dryer (Heto FD3, Heto-Holten A/S, Denmark), and NMR spectrometer (GSX400, JEOL, Japan).

Determination of ionization constants (pK_as)

By UV absorption spectrophotometry A stock methanolic solution of **Cisp** (1.0 mM) was diluted further with 0.05 M citrate buffers of different pHs ranging from 2 to 12 to obtain final solutions having fixed concentration of 0.02 mM. The absorbencies of these solutions were measured using first derivative UV/visible spectrophotometry at 283 nm.

By pH solubility profile Excess amounts of **Cisp** were added to 50 ml of 0.05 M citrate buffers with pH ranging from 2 to 12. The samples were mechanically shaken in a thermostatic bath shaker at 30°C for 2 days, an aliquot was filtered using a 0.45 μm filter (cellulose acetate or cellulose nitrate, Advantec MFS Inc., Duplin, USA). The **Cisp** content was determined using first derivative UV spectrophotometry at 283 nm. The pK_as were estimated according to procedures discussed earlier [6].

Phase solubility studies

Solubility studies were performed as described by Higuchi and Connors [10]. Excess amounts of **Cisp** were added to 50 ml of the desired aqueous β-CD solutions ranging in concentration from 0 to 18 mM. The samples were mechanically shaken in a thermostatic bath shaker at constant temperature to attain equilibrium (2 days) and let to settle for 24 h, an aliquot was filtered using a 0.45 μm filter. The pH of the filtrate was measured by calibrated pH-meter. The drug assay was conducted using first derivative spectrophotometry at 283 nm. Moreover, the complex formation constants were estimated as described earlier [11].

Quantitation of hydrophobic effect

A quantitative measure of the contribution of the hydrophobic effect (desolvation) to complex formation was obtained from the linear variation of the free energy of 1:1 complex formation ($\Delta G_{11} = -RT \ln K^x_{11} < 0$) with the free energy of inherent drug solubility ($\Delta G_{S_o} = -RT \ln S^x_o > 0$) obtained in 0.05 M citrate buffer at different pHs (the superscript (x) denotes the mole fraction standard state) [5, 6, 12]. For example, if ΔG_{11} varies linearly with ΔG_{S_o}, then the magnitude of the negative slope of the linear plot would indicate the fraction of the driving force for complex formation contributed by the hydrophobic

character of the guest molecule (**Cisp**). On the other hand, the intercept would provide a measure of the contribution (in kJ/mol) of other factors, including specific interactions, to complex stability.

^{1}H-Nuclear magnetic resonance

Samples of β-CD and the hydrochloride salts of **Cisp** and the complex were dissolved in 99.98% D_2O and filtered before use. The 400 MHz ^{1}H-NMR spectra were obtained at 25°C. Chemical shifts are quoted relative to sodium 3-trimethylsilyl [D_4] propionate at 0.0 ppm, but spectra were calibrated via the known position of the residual HOD resonance, which was used as a reference.

Molecular modeling

Molecular modeling simulations of **Cisp**/β-CD interactions in vacuo were performed using the Hyperchem® molecular modeling (release 6.03 professional, Hypercube Inc., Waterloo, Canada). Both Amber and enhanced MM Force fields implementing the atomic charges or bond dipoles options for calculation of electrostatic interactions were used in these computations. Partial atomic charges were obtained by means of AM1 semi-empirical calculations [13]. Energy minimization was performed using the conjugate gradient algorithm (0.01 kcal/mol Å gradient). The initial molecular geometry of β-CD was obtained using X-ray diffraction data [14–17], which was then energetically optimized using the Amber force field by imposing a restraint on the dihedral angles to the average values [16]. The **Cisp** molecule was built up from standard bond lengths and bond angles, which was further optimized with the Amber and MM force fields.

The previously optimized structures of **Cisp** and β-CD molecules were allowed to approach each other along the symmetric x-axis passing through the center of the β-CD cavity. The fluorophenyl side of **Cisp** was allowed to approach through both the wide and narrow rims of β-CD cavity. The energy of **Cisp** was computed (while β-CD was fixed) at 1 Å intervals, starting at x = –20 Å all through x = + 20 Å from the origin of the Cartesian coordinate, which was designated by the center of the ether glucoside oxygen atoms of β-CD and an atom closest to the center of mass of the **Cisp** molecule. The binding energy ($E_{\text{binding}} = E_{\text{complex}} - \sum E_{\text{components}}$) was plotted against x for each longitudinal approach to indicate the energy minima. The whole **Cisp**/β-CD system of minimum energy thus obtained was allowed to interact free of restrictions to either molecule to obtain the optimized 1:1 complex configuration whose energy was computed together with the van der Waals and electrostatic contributions.

To obtain the optimized 1:2 **Cisp**/β-CD complex configuration, the already optimized 1:1 complex was allowed to approach from the fluorophenyl side through either rim of a second β-CD molecule. The binding energy corresponding to the optimized configuration was similarly arrived at free of restrictions as discussed above. It should be noted that the energetics of **Cisp**/β-CD interaction were simulated for neutral **Cisp** in vacuo, where protonated **Cisp** and water molecules were ignored to save computational time especially for large molecules [18].

Results and discussion

Ionization constants (pK_as)

Analysis of the variation of the first derivative UV absorptivity of a fixed concentration of **Cisp** (0.02 mM) at 283 nm with pH (Fig. 1a) yielded the pK_{a1} value of 8.7

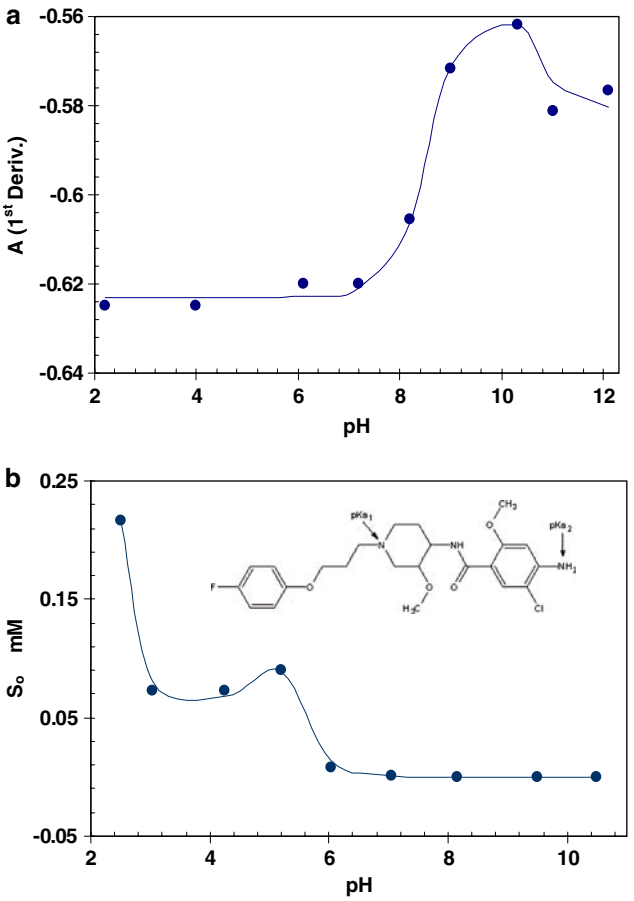

Fig. 1 (**a**) First derivative UV absorbencies of **Cisp** at fixed concentration (0.02 M) at 283 nm against pH, and (**b**) pH solubility profile of **Cisp**, both obtained in 0.05 M citrate buffer at 30°C

(piperidine moiety) and $pK_{a2} < 2$ (aniline moiety). The corresponding-analysis of the variation of inherent **Cisp** solubility (S_o) with pH (Fig. 1b) yielded estimates of pK_{a1} at 8.2 and $pK_{a2} < 2$. The solubility of **Cisp** was found to be limited by the solubility product of the **Cisp**H^+ citrate^{1-} salt at low pH (pH range 3–5.2) where pK_{sp} was estimated at 3.0. The value of 8.7 estimated for pK_{a1} from the UV absorption method is to be considered more accurate since a very dilute solution of **Cisp** was used where no salt saturation takes place at low pH.

Phase solubility diagrams and the hydrophobic effect

The phase solubility diagrams of **Cisp** against β-CD at 30°C were obtained at different pHs (Fig. 2a). The corresponding inherent solubilities (S_o) of **Cisp** and complex formation constants (K_{11} and K_{12}) are listed in Table 1. The results indicate that K_{11} decreases as S_o increases while pH decreases. In contrast, K_{12} is apparently less sensitive to variation in S_o (note how K_{11} increases from 110 to 20 000 M^{-1} as pH rises from 2.6 to 12.2). This indicates a significant contribution of the hydrophobic effect (dissolvation) towards 1:1 complex stability [5, 6, 12]. A quantitative estimate was obtained from the linear plot of free energy of 1:1 complex formation ($\Delta G^o_{11} = -RT \ln K^x_{11}$) against the free energy of inherent **Cisp** solubility ($\Delta G^o_{S_o} = -RT \ln S^x_o$) (Fig. 2b). The slope (–0.35) indicates that only 35% of the total driving force for complex for-

Table 1 Complex formation parameters for **Cisp**/β-CD system in water and in 0.05 M citrate buffer at different pHs and 30°C

pH	$S_o \times 10^3$ (mM)	K_{11} (M^{-1})	K_{12} (M^{-1})
Water (6.1)	5.0	520	20
2.6	220	110	64
6.0	9.93	236	30
12.2	0.053	20 000	20

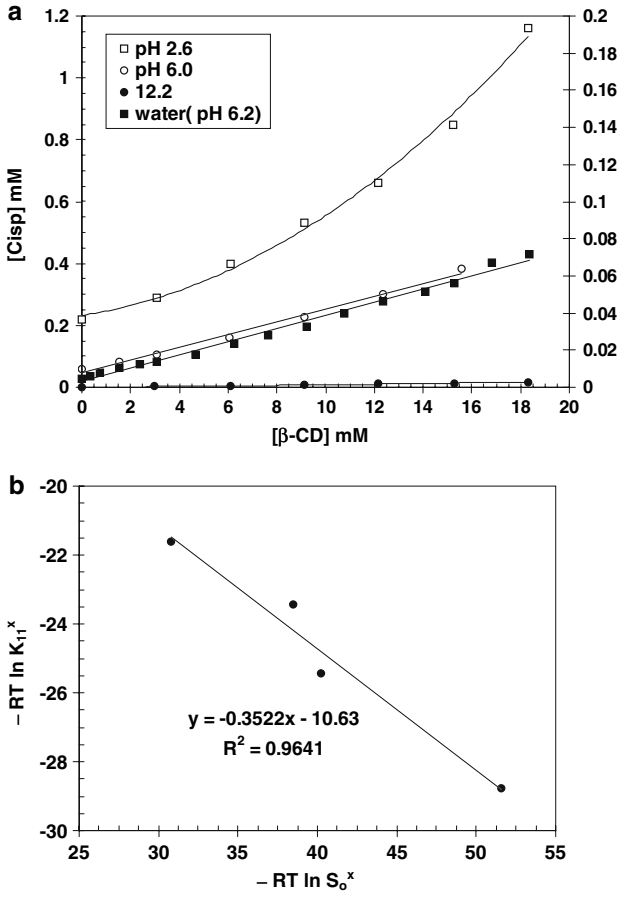

Fig. 2 (**a**) Phase solubility diagrams of the **Cisp**/β-CD system in water and in 0.05 M citrate buffer at 30°C at different pHs (the left *y*-axis corresponds to pH 2.6) and (**b**) A plot of $-RT \ln K^x_{11}$ against $-RT \ln S^x_o$ (*x* denotes the mole fraction standard state)

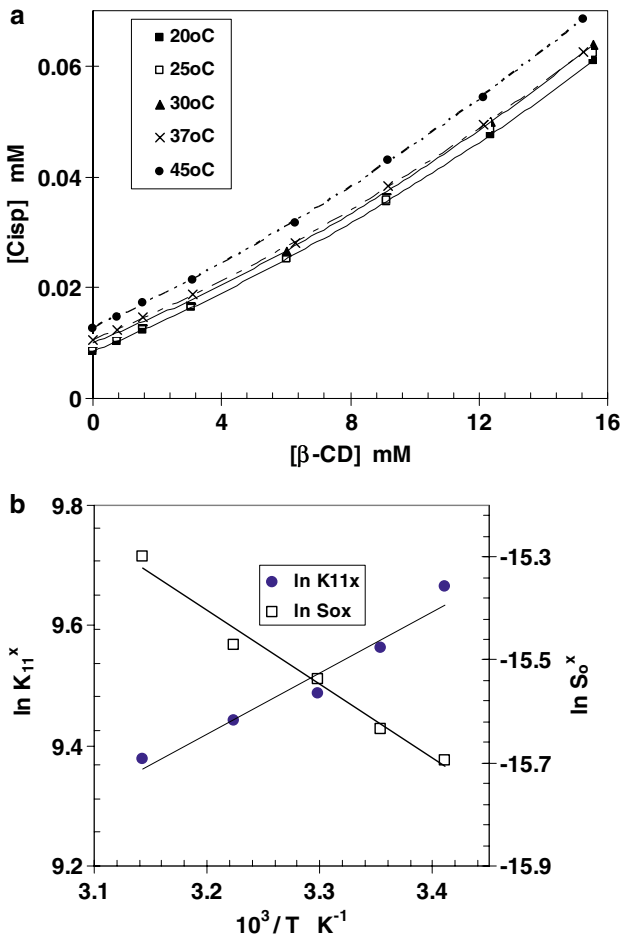

Fig. 3 (**a**) Phase solubility diagrams of **Cisp**/β-CD obtained in 0.05 M citrate buffer (pH 6.0) at different temperatures, and (**b**) the corresponding van't Hoff plots of $\ln K^x_{11}$ and $\ln S^x_o$ against $1/T$ (*x* stands for the mole fraction standard state)

Table 2 Complexation parameters of **Cisp**/β-CD obtained in 0.05 M citrate buffer at pH 6.0 and different temperatures (Fig. 3), and the corresponding standard thermodynamic functions corresponding to the inherent solubility (S_o) of **Cisp** and to 1:1 **Cisp**/β-CD complex formation in 0.05 M

T °C	$S_o \times 10^3$ (mM)	K_{11} (M^{-1})	K_{12} (M^{-1})
20	8.47	284	26
25	9.00	257	31
30	9.93	236	30
37	10.6	227	28
45	12.6	213	25
Parameter	Inherent **Cisp** solubility ($S_{o)}$		1:1 **Cisp**/β-CD complex formation
ΔH^o (kJ/mol)	12		-9
ΔS^o (J/mol.K)	–90		51
ΔG^o (kJ/mol)	39		-24
S_o^o (mM)	0.00906		
K_{11}^o (M^{-1})	260		

mation is contributed by the hydrophobic character of **Cisp**. The intercept (–10.6 kJ/mol), on the other hand, indicates the contribution of other factors, including specific interactions to complex stability.

Thermodynamics of complex formation

Figure 3a depicts the PSDs of **Cisp**/β-CD obtained in 0.05 M citrate buffer at pH 6.0 and different temperatures (20–45°C). Estimates of the complex formation constants are listed in Table 2. From the Van't Hoff plot of ln K_{11}^x and ln S_o^x against $1/T$ (Fig. 3b), the corresponding thermodynamic parameters were obtained and are also listed in Table 2. Obviously, protonated 1:1 **Cisp**/β-CD complex formation in aqueous solution ($\Delta G_{11}° = -24$ kJ/mol) is stabilized by favorable enthalpy ($\Delta H_{11}° = -9$ kJ/mol) and entropy ($\Delta S_{11}° = 50$ J/mol K). In contrast, the inherent solubility (S_o) of **Cisp** in water ($\Delta G° = 39$ kJ/mol) is impeded by unfavorable enthalpy change ($\Delta H° = 12$ kJ/mol) and also unfavorable entropy change ($\Delta S° = -90$ J/mol K).

^{1}H-Nuclear magnetic resonance and molecular modeling

The ^{1}H-NMR spectra of **Cisp**·HCl, β-CD and their corresponding complex in deuterium oxide showed

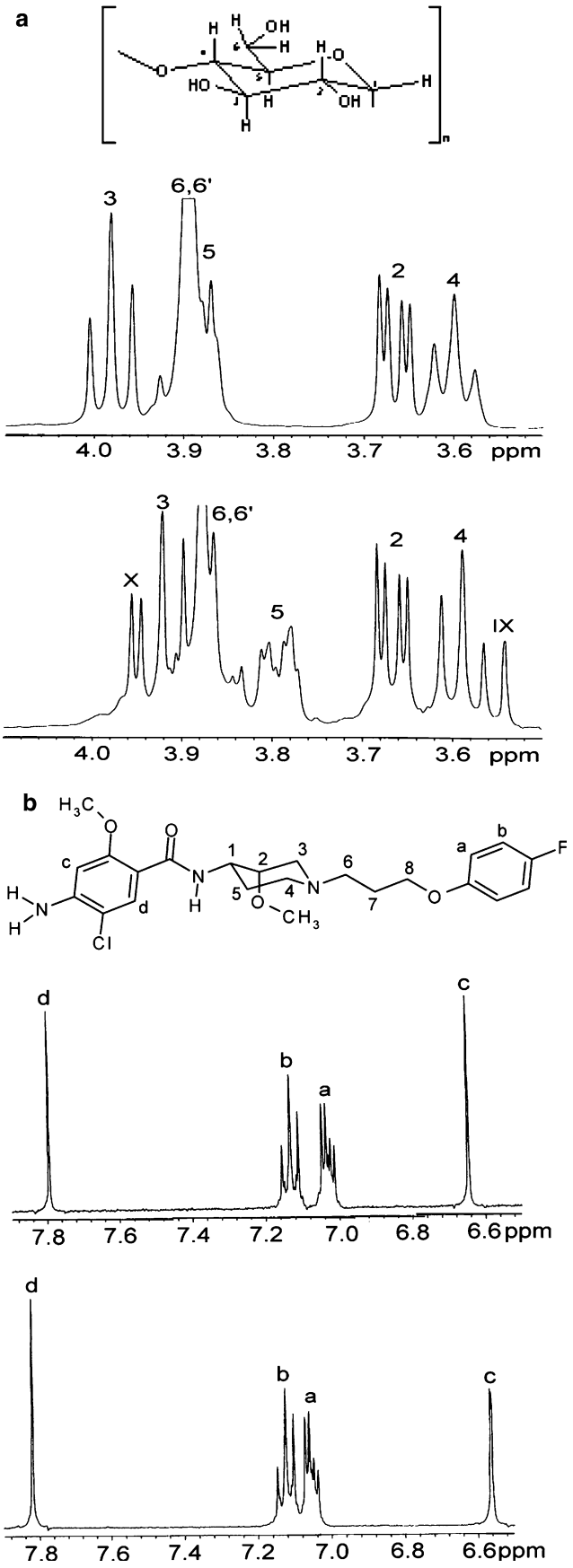

Fig. 4 400 MHz ^{1}H-NMR spectra of the **Cisp**·HCl/β-CD system in D_2O at 25°C (**a**) for β-CD and (**b**) for aromatic protons of **Cisp**·HCl. The upper and lower traces correspond to the compound before and after complexation, respectively

that the upfield chemical shift displacement ($\Delta\delta$) on complexation are highest for inner cavity protons H_3 (–0.054 ppm) and H_5 (–0.098 ppm) of β-CD, thus indicating **Cisp**/β-CD inclusion complex formation. Protons H_1, H_2, H_4 and $H_{6,6'}$ demonstrate less $\Delta\delta$ values (–0.014 to 0.005 ppm) on complexation (Fig. 4A).

For the piperidine and propoxy groups of **Cisp**, all protons showed downfield $\Delta\delta$ values (0.005–0.039 ppm), while protons of methoxy groups attached to the piperidine and aminophenyl moieties showed less significant downfield $\Delta\delta$ (0.005–0.015 ppm). Aromatic protons exhibit upfield and downfield chemical shift displacements thus indicating that protons of the same aromatic ring experience different microenvironments (Fig. 4B). For example, proton d showed a downfield $\Delta\delta$ (0.025 ppm), while proton c exhibits a more significant upfield $\Delta\delta$ (–0.085 ppm). The same is also observed for protons a (0.017 ppm) and b (–0.009 ppm), which suggests that both phenyl moieties are either partially included leaving some protons (b and c) more shielded by the hydrophobic β-CD cavity, while protons a and d are deshielded by exposure to the hydroxyl group networks situated on either side of the β-CD cavity, or all four protons experiencing different microenvironments imposed by amine, amide and propoxy groups hydrogen bonded to β-CD hydroxyls. The results also indicate that some of the piperidyl and propoxy protons are slightly shielded while others are deshielded, thus indicating either the presence of isomeric complexes, or complexes of different stoichiometries in solution. Formation of 1:1 and 1:2 **Cisp**/β-CD complexes was proved from rigorous analysis of the phase solubility diagrams (Figs. 2a and 3a, Tables 1 and 2). Therefore, the presence of a mixture of 1:1 and 1:2 complexes in solution would produce ^{1}H-NMR spectra where neighboring protons of complexed **Cisp** exhibit opposite and different chemical shift displacements due to whether they are located within the hydrophobic β-CD cavity, near the rim of the cavity, or somewhere in between the opposite rims of two β-CD molecules in a 1:2 **Cisp**/β-CD complex configuration. Figure 5 shows the solution composition in terms of 1:1 and 1:2 complex concentrations corresponding to a phase solubility diagram obtained in 0.05 M citrate buffer at pH 6.0 and 25°C.

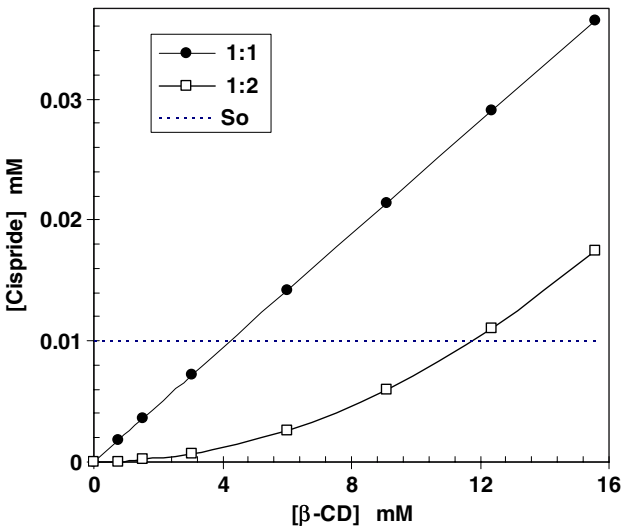

Fig. 5 Variation of the 1:1 and 1:2 **Cisp**/β-CD complex concentrations with β-CD concentration corresponding to a phase solubility diagram obtained in 0.05 M citrate buffer at pH 6.0 and 25°C

Molecular modeling in vacuo

Molecular mechanical modeling of the interaction of **Cisp** with β-CD in vacuo was conducted for the two possible approaches of the fluorophenyl side of **Cisp** through the wide and narrow rims of β-CD. The energetically optimized configurations corresponding to 1:1 complex stoichiometry indicate complete inclusion of the amide and partial inclusion of the piperidine moiety. Another almost equally probable optimized configuration is formed by partial inclusion of the piperidine and complete inclusion of the propoxy moiety. It was observed that the presence of the methoxy group attached to position 3 of the piperidine moiety inhibits complete inclusion of this moiety. A side view of the most probable optimized 1:1 complex configuration is depicted in Fig. 6a. A corresponding side view of the optimized 1:2 **Cisp**/β-CD complex is depicted in Fig. 6b. In this configuration, the aminophenyl and propoxy groups appear completely included within the cavities of two opposite β-CD molecules. The two hydroxyl group networks located at the wide rims of the two opposing β-CD molecules seem to envelop the piperidine and amide moieties in between. The driving force for 1:1 and 1:2 complex formation, in vacuo, is predominantly van der Waals, with very little contribution from electrostatic effects.

Conclusion

Cisp forms soluble complexes of 1:1 and 1:2 **Cisp**/β-CD complex stoichiometry. The 1:1 complex formation constant (K_{11}) is highly sensitive to pH, where K_{11} increases as pH increases in an opposite trend to that of the inherent **Cisp** solubility (S_o). Linear free energy correlations indicate that hydrophobic effects (desolvation) contribute about 35% of the driving force for

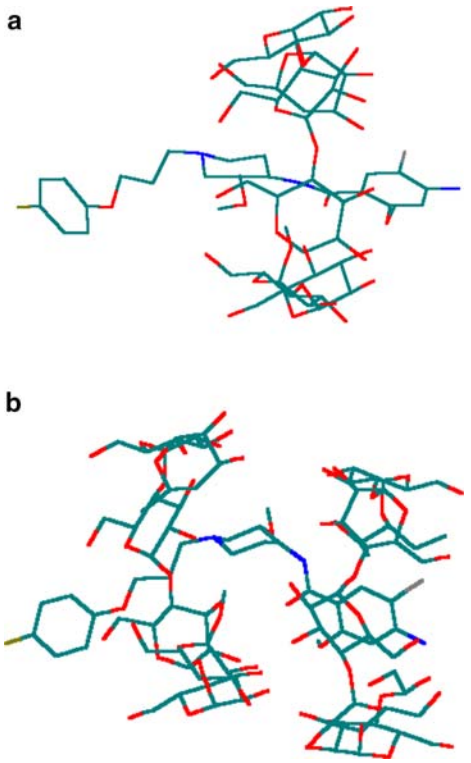

Fig. 6 Side view of the optimized configurations of (**a**) 1:1 **Cisp**/β-CD and (**b**) 1:2 **Cisp**/β-CD complexes

Cisp/β-CD complex formation in aqueous solution. In contrast, the contribution of other factors, including specific interactions amount to –10.6 kJ/mol. It was found that complex formation for protonated **Cisp** is driven by favorable enthalpy and entropy changes. ^{1}H-NMR and molecular mechanical studies indicate the possible formation of isomeric 1:1 and 1:2 **Cisp**/β-CD inclusion complexes.

References

1. Loftsson, T., Brewster, M.E.: Pharmaceutical applications of cyclodextrins. 1. Drug solubilization and stabilization. J. Pharm. Sci. **85**(10), 1017–1025 (1996)
2. Stella, V.J., Rajewski, R.A.: Cyclodextrins: their future in drug formulation and delivery. Pharm. Res. **14**(5), 556–567 (1997)
3. Menard, F.A., Dedhiya, M.G., Rhodes, C.T.: Physicochemical aspects of the complexation of some drugs with cyclodextrins. Drug Dev. Ind. Pharm. **16**(1), 91–113 (1990)
4. Backensfeld, T., Muller, B.W., Kolter, K.: Interaction of NSA with cyclodextrins and hydroxypropyl cyclodextrin derivatives. Int. J. Pharm. **74**(2–3), 85–93 (1991)
5. Al Omari, M.M., Zughul, M.B., Davies, J.E.D., Badwan, A.A.: Effect of buffer species on the inclusion complexation of acidic drug celecoxib with cyclodextrin in solution. J. Incl. Phenom. Macrocyc. Chem. **55**(3–4), 247–254 (2006)
6. Al Omari, M.M., Zughul, M.B., Davies, J.E.D., Badwan, A.A.: Sildenafil/cyclodextrin complexation: stability constants, thermodynamics, and guest-host interactions probed by ^{1}H-NMR and molecular modeling studies. J. Pharm. Biomed. Anal. **41**(3), 857–865 (2006)
7. Rekharsky, M.V., Goldberg, R.N., Schwarz, F.P., Tewari, Y.B., Ross, P.D., Yamashoji, Y., Inoue, Y.: Thermodynamic and nucler magnetic resonance study of the interactions of alpha- and beta-cyclodextrin with model substances: phenethylamine, ephedrines, and related substances. J. Am. Chem. Soc. **117**, 8830 (1995)
8. Muller, B.W., Albers, E.: Complexation of dihydropyridine derivatives with cyclodextrins and 2-hydroxypropyl-β-cyclodextrin in solution. Int. J. Pharm. **79**(2–3), 273–288 (1992)
9. Esclusa-Diaz, M.T., Gayo-Otero, M., Perez-Marcos, M.B., Vila-Jato, J.L., Torres-Labandeira, J.J.: Preparation and evaluation of ketoconazole-β-cyclodextrin multicomponent complexes. Int. J. Pharm. **142**(2), 183–187 (1996)
10. Higuchi, T., Connors, K.A.: Phase-solubility techniques. Advan. Anal. Chem. Instr. **4**, 117–212 (1965)
11. Zughul, M.B., Badwan, A.A.: SL_2 type phase solubility diagrams, complex formation and chemical speciation of soluble species. J. Incl. Phenom. Mol. Recog. Chem. **31**(3), 243–264 (1998)
12. El-Barghouthi, MI., Masoud, N.A., Al-Kafawein, J.K., Zughul, M.B., Badwan, A.A.: Hostguest interactions of risperidone with natural and modified cyclodextrins: phase solubility, thermodynamics and molecular modeling studies. J. Incl. Phenom. Macrocyc. Chem. **53**(1–2), 15–22 (2005)
13. Dewar, M.J.S., Zoebisch, E.G., Healy, E.F., Stewart, J. J.P.: Development and use of quantum mechanical molecular models. 76. AM1: a new general purpose quantum mechanical molecular model. J. Am. Chem. Soc. **107**(13), 3902–3909 (1985)
14. Puliti, R., Mattia, C.A., Paduano, L.: Crystal structure of a new alpha-cyclodextrin hydrate form. Molecular geometry and packing features: disordered solvent contribution. Carbohydr. Res. **310**(1–2), 1–8 (1998)
15. Linder, K., Saenger, W.: Topography of cyclodextrin complexes. Part XVII. Crystal and molecular structure of cycloheptaamylose dodecahydrate. Carbohydr. Res. **99**(2), 103–115 (1982)
16. Saenger, W., Jacob, J., Gessler, K., Steiner, T., Hoffman, D., Sanbe, H., Koizumi, K., Smith, S.M., Takaha, T.: Structures of the common cyclodextrins and their larger analogues-beyond the doughnut. Chem. Rev. **98**(5), 1787–1802 (1998)
17. Harata, K.: The structure of the cyclodextrin complex. XX. Crystal structure of uncomplexed hydrated β-cyclodextrin. Bull. Chem. Soc. Jpn. **60**(8), 2763–2767 (1987)
18. Tong, W., Lach, J.L., Chin, T., Guillory, J.K.: Structural effects on the binding of amine drugs with the diphenylmethyl functionality to cyclodextrins. II. A molecular modeling study. Pharm. Res. **8**(10), 1307–1312 (1991)